72-hour Time Series Forecasting of Hourly Relativistic Electron Fluxes at Geostationary Orbit by Deep Learning

Jihyeon Son[1], Yong-Jae Moon[1,2], and Seungheon Shin[1]

[1]School of Space Research, Kyung Hee University, Yongin, 17104, Republic of Korea

[2]Department of Astronomy and Space Science, Kyung Hee University, Yongin, 17104, Republic of Korea,

Key Points:

- A deep learning model based on multilayer perceptron is presented to forecast hourly relativistic (>2 MeV) electron fluxes at geostationary orbit for the next 72 hours.
- The performance of our model is much better than that of previous studies in view of metrics such as prediction efficiency, root mean square error, and correlation coefficient.
- Our model successfully predicts the change of electron fluxes such as diurnal variation and sudden increase.

Corresponding author: Yong-Jae Moon, moonyj@khu.ac.kr

Abstract

In this study, we forecast hourly relativistic ($>$ 2 MeV) electron fluxes at geostationary orbit for the next 72 hours using a deep learning model. For this we consider three deep learning methods, such as multilayer perceptron (MLP), LSTM, and sequence-to-sequence based on LSTM. The input data of the model are solar wind parameters (temperature, density and speed), interplanetary magnetic field ($|B|$ and B_z), geomagnetic indices (Kp and Dst), and electron fluxes themselves. All input data are hourly averaged ones for the preceding 72 consecutive hours. We use electron flux data from GOES-15 and -16, and perform cross-calibration to match the two data. Total period of the data is from 2011 January to 2021 March (GOES-15 data for 2011-2017 and GOES-16 data for 2018-2021). We divide the data into training set (January-August), validation set (September), and test set (October-December) to consider the solar cycle effect. Our main results are as follows. First, the MLP model, which is the best, successfully predicts hourly electron fluxes for the next 72 hours. Second, root-mean-square error (RMSE) of our model is from 0.18 (for 1h prediction) to 0.68 (for 72h prediction), and prediction efficiency (PE) is from 0.97 to 0.53, which are much better than those of the previous studies. Third, our model well predicts both diurnal variation and sudden increases of electron fluxes associated with fast solar winds and interplanetary magnetic fields. Our study implies that the deep learning model can be applied to forecasting long-term sequential space weather events.

Plain Language Summary

Relativistic electron fluxes (>2 MeV) can damage satellites, resulting in loss of function. Thus, forecasting electron fluxes is a necessary task to minimize the loss. We develop a deep learning model to perform time-series forecasting of hourly relativistic electron fluxes 3 days ahead. For this, we use solar wind parameters, interplanetary magnetic field, geomagnetic indices, and electron fluxes from GOES-15 and 16. Our model shows outstanding performances for time series forecasting of electron fluxes in view of metrics. In addition, our model successfully predicts the change of electron fluxes such as diurnal variation and sudden increase.

1 Introduction

There have been a lot of spacecraft in geostationary orbit (GEO) for various objectives such as communications, navigation and meteorology. They are constantly exposed to the dangers by high-energy electrons called "killer electrons". They can cause deep dielectric charging by burying themselves in dielectric materials. If the accumulated charge becomes high enough, a powerful discharge can occur. It may cause physical damage to the satellites, resulting in temporary or permanent loss of function (Baker, 2000; Horne et al., 2013; Baker et al., 2018). For this reason, the prediction of electron fluxes in GEO is essential to minimize the loss.

There have been many studies to predict electron fluxes using various methods. Baker et al. (1990) used the method of linear prediction filter (LPF) analysis to characterize and predict the general relation between solar wind or geomagnetic indices and electron properties. The relativistic electron forecast model operated by Space Weather Prediction Center (SWPC) is based on this method. Physics based models (Li et al., 2001; Li, 2004; Turner & Li, 2008; Lyatsky & Khazanov, 2008), empirical models and statistical models (Ukhorskiy et al., 2004; Miyoshi & Kataoka, 2008; H. L. Wei et al., 2011; Denton et al., 2015; Boynton et al., 2016) have been also suggested. In addition, neural network based models have been proposed since the early 1990s for forecasting electron fluxes. (Koons & Gorney, 1991; Fukata et al., 2002; Ling et al., 2010; Shin et al., 2016).

Deep learning, one of the neural network methods, is a method to solve complex non-linear problems. For forecasting electron fluxes, there have been a few attempts to apply deep learning methods. L. Wei et al. (2018) used a long short term memory (LSTM) method (Hochreiter & Schmidhuber, 1997) to predict daily > 2 MeV electron integral flux 1 day ahead at geostationary orbit. Zhang et al. (2020) made a multilayer perceptron model with two hidden layers and scaling transformation layer to predict average daily relativistic electron fluxes. They combined the model with the quantile regression method to predict in probabilistic approach. The prediction efficiency of their studies shows from about 0.8 to 0.9, which implies that the deep learning method shows good performance in predicting electron fluxes.

Most of the previous studies aim to predict the electron flux at a certain time in the future. On the other hand, in this study, we develop hourly forecast models with the next 72 hours time-series data by deep learning. For this we apply three methods, such

as multilayer perceptron (MLP), LSTM, and sequence-to-sequence based on LSTM (Sutskever et al., 2014). This paper is organized as follows. We introduce detailed explanations of our data and models in Section 2 and 3, respectively. We evaluate our best model with metrics and show the results in Section 4. Finally, we summarize our study in section 5.

2 Data

For this study, we use 5-minute averaged > 2 MeV electron flux data observed from Geostationary Operational Environmental Satellite (GOES) 15 and 16. GOES-15 was operated from 2011 to 2020 March, and GOES-16 has been in service since 2018. Because the data are observed by different satellites, we need to calibrate these two kinds of data. For the data cross-calibration, we average the data over an hour, and then take a logarithm of them. We find a 4th-order fitting function using the data in the overlapping periods (2018-2020 March), and fit GOES-15 data to GOES-16 data. Figure 1 shows the distribution between the data from two satellites before and after calibration. After calibration, the data distribution becomes close to the one-to-one line (the red dashed line). In other words, it has higher consistency than before. We use the calibrated GOES-15 data from 2011 to 2017, and GOES-16 data from 2018 to 2021 March in this study.

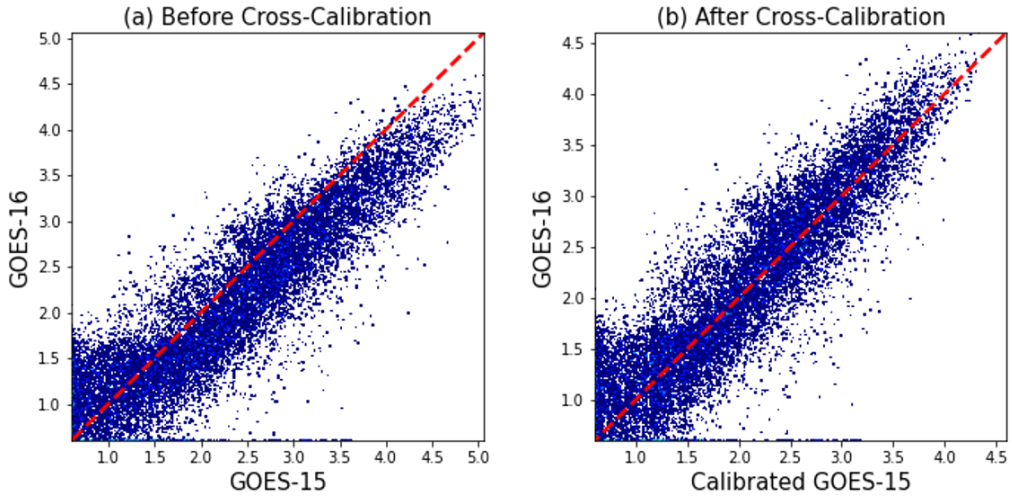

Figure 1. Data distribution between GOES-15 and GOES-16 data (2018-2020 March). (a) shows data distribution before cross-calibration, and (b) shows after cross-calibration. The red dashed line is a one-to-one line ($y = x$).

We use solar wind data (density, speed, and temperature), interplanetary magnetic field ($|B|$ and B_z), Dst index, and Kp index as input data of our model. These data are obtained from OMNIWeb service of the Space Physics Data Facility at the Goddard Space Flight Center (https://omniweb.gsfc.nasa.gov/) as 1 hour resolution. For the Kp index, the daily sum of data are used instead of hourly data (Ling et al., 2010) since they give better results. We also use electron fluxes themselves as input data.

The variation of electron fluxes shows both short-term (diurnal and solar-rotational) and long-term (annual and solar cycle) periodicity (Baker et al., 1993). We consider the solar cycle effect as the most important cause of change of the electron fluxes, so we divide the total data which cover one solar cycle into as follows: every January-August data for the training set, every September for the validation set, and every October-December for the test set.

3 Method

We make three deep learning models for this work. The models we develop are MLP model, LSTM model, and sequence-to-sequence model based on LSTM. Among them, the MLP model shows the best results in view of metrics such as prediction efficiency and root mean square, so we introduce this model hereafter.

Multi layer perceptron is a basic model structure of deep learning, which consists of an input layer, several hidden layers, and an output layer. MLP is also called "feed-forward neural network", which means the signal from the input layer flows in the forward direction to the output layer. The error between the predicted values and the target values goes back to the beginning of the network, and the weights of each node are updated to minimize this error. This mechanism is called "back propagation" (Rumelhart et al., 1986). The error is calculated by a loss function (or cost function). By repeating feed-forwarding and back propagation, the model is trained.

Figure 2 shows the architecture of our model. Inputs are the data introduced in section 2 from t-71 to t, and outputs are the electron fluxes from t+1 to t+72, where t is prediction time. Our model consists of 4 dense layers (or fully connected layers), which are connected to all nodes of the next layers. In Figure 2, the number in parentheses means the number of nodes in each layer. The electron flux data and the other data are entered separately to two dense layers. By doing this, we expect the model to learn that the tar-

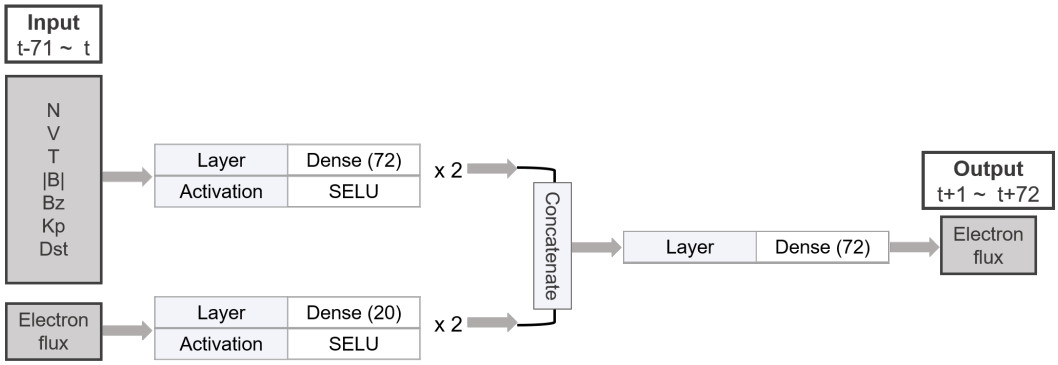

Figure 2. Architecture of our model. The electron flux data and the other data such as solar wind parameters and geomagnetic indices are separately entered as input. Each of the input passes through two dense layers, and is then combined. The electron fluxes are predicted from the concatenated layer.

get is the same kind of data as the separately entered data, and easily to capture the pattern of electron fluxes. Each of the input passes through two dense layers, and is then concatenated at the end of the network. From the combined layer, the model finally predicts the target electron fluxes. Each of the dense layer is followed by an activation function named 'Scaled Exponential Linear Unit (SELU)' (Klambauer et al., 2017). The SELU activation induces self-normalizing properties like variance stabilization, which in turn avoids exploding and vanishing gradients that interrupt the learning of the model. It is given by

$$\mathrm{selu}(x) = \lambda \begin{cases} x & \text{if } x > 0 \\ \alpha e^x - \alpha & \text{if } x \leq 0 \end{cases}, \tag{1}$$

where $\alpha \approx 1.6733$ and $\lambda \approx 1.0507$ (Klambauer et al., 2017). After trying to apply several activation functions, we find that the SELU is the most suitable for our model. As a loss function, we define weighted mean squared error (WMSE), which is given by

$$\begin{aligned} \mathrm{WMSE} &= \omega \textstyle\sum_{i=1}^{N} (f_i - y_i)^2 \\ \omega &= \frac{k}{\sum_{i=1}^{6} i} \quad (k = 1, 2, ..., 6), \end{aligned} \tag{2}$$

where f_i, y_i, and ω denote the i-th predicted value, target value, and weight, respectively. k is a value depending on the time range of the output value. For example, for the data from t+1 to t+6, $k = 6$, and for the data from t+67 to t+72, $k = 1$. Since we think it is most important to predict values in the near future, we expect that the closer to the prediction time, the better the prediction if we give a bigger weight. As an optimizer for the model, we use 'Adaptive Moment Estimation (Adam)' (Kingma & Ba, 2014) optimizer with the learning rate of 5×10^{-5}.

4 Results and Discussions

Our model predicts > 2 MeV electron fluxes for the next 72 hours with the input data of the previous 72 hours. Figure 3 shows two examples of results by our model. The red dashed line is prediction time (t). The left values of the prediction time are the data of input time sequences (t-71 $\sim$ t), and the right values are ones of output time sequences (t+1 $\sim$ t+72). The blue lines and yellow lines are the observed electron fluxes and the predicted ones by our model, respectively. The electron fluxes in GEO show diurnal variance that is observed high near local noon and low near local midnight due to the magnetospheric magnetic field (Onsager et al., 2002). As seen in Figure 3(a), which shows when the electron fluxes are almost steady, the model seems to have learned the periodicity well. Figure 3(b) shows when the electron fluxes suddenly increase. Although the prediction values slightly different from the target values at the beginning of prediction, we can see that the model successfully predicts the increasing phase.

Why the model is so good at predicting changes in electron fluxes seems to be due to that the input data we use are closely related to the electron flux data (Vassiliadis et al., 2002; Li, 2004; Reeves et al., 2011; Hartley et al., 2014; Zhang et al., 2020; Katsavrias et al., 2021). For verifying that the input data really help the model to predict well, we make a baseline model which has only electron flux data as input. In Figure 4, we show a result of the baseline model (Figure 4(a)) and our model (Figure 4(b)) at the same time. The baseline model has learned the diurnal periodicity of electron fluxes, but its prediction almost maintains the input values like the persistence model. On the other hand, our model, which has additional input data, successfully predicts rapid changes in electron fluxes. By comparing these two models, it can be seen that the input data for the model are used appropriately to predict the changes in electron fluxes, which is consistent with the understanding obtained from previous studies.

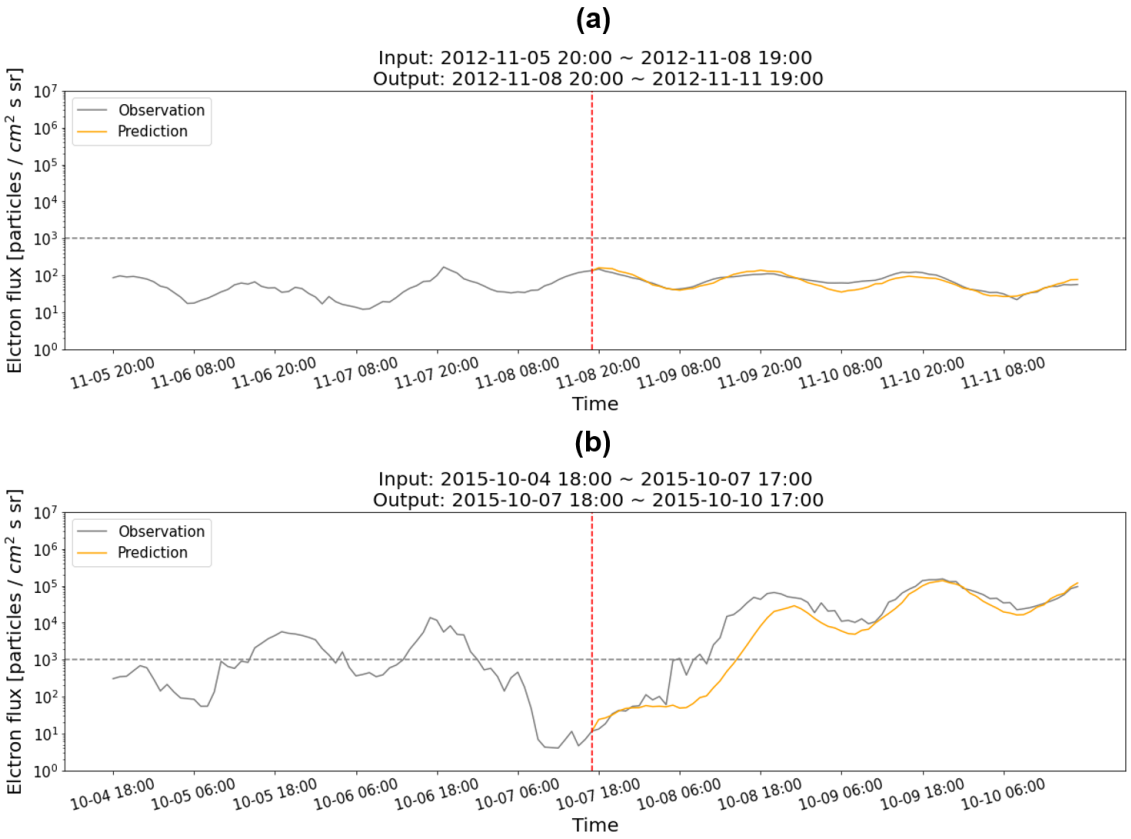

Figure 3. Two examples of the result of our model. Based on the red dashed line (prediction time), the left is the input time sequences and the right is the output time sequences. The gray lines are observed electron flux values, and the yellow lines are predicted ones by our model.

To evaluate our model quantitatively, we calculate prediction efficiency (PE) and root-mean-square error (RMSE), which are given by

$$PE = 1 - \frac{\sum(y_i - f_i)^2}{\sum(y_i - \bar{y})^2} \tag{3}$$

and

$$RMSE = \sqrt{\frac{1}{N}\sum_{i=1}^{N}(y_i - f_i)^2}, \tag{4}$$

where f_i, y_i and $\bar{y}$ are the i-th predicted value, target value, and the average of the target values, respectively. PE indicates better performance as it is closer to 1, and RMSE shows as it is closer to 0. The results are obtained using only the test set data mentioned in Section 2. Figure 5 shows values of PE and RMSE of our model for each time step. It is noted that we calculate the scores with log-scaled electron flux values. As seen in Figure 5, the results for 1 hour prediction show almost perfect scores. Naturally, the scores

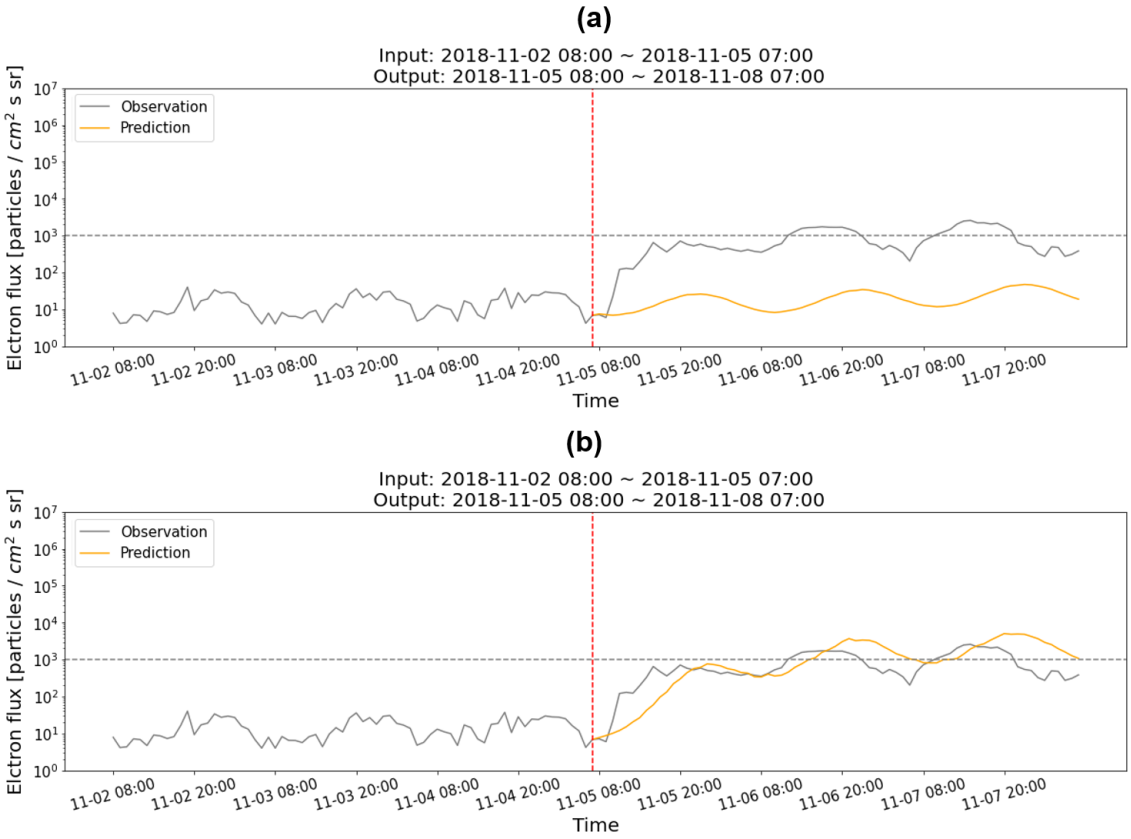

Figure 4. (a) is a result of a baseline model with single input (electron flux data), and (b) is a result of our model. The gray lines are observed electron flux values, and the yellow lines are predicted ones by the models.

get worse as the prediction time goes, but the score for the 72-hour prediction shows still good performance.

Table 1 shows the prediction efficiency of our model compared with other hourly forecasting models: previous ones (Shin et al., 2016; Qian et al., 2020) and a persistence model. The persistence model is a model in which the input data of the last time become the predicted values. Our model shows 0.97 and 0.78 in 1-hour ahead and 24-hour ahead prediction, respectively, which are the highest PE among those models. On the other hand, there have been also several models that predict the daily average data (Lyatsky & Khazanov, 2008; Ling et al., 2010; L. Wei et al., 2018; Zhang et al., 2020), but we cannot directly compare our model with these studies because of different time resolution.

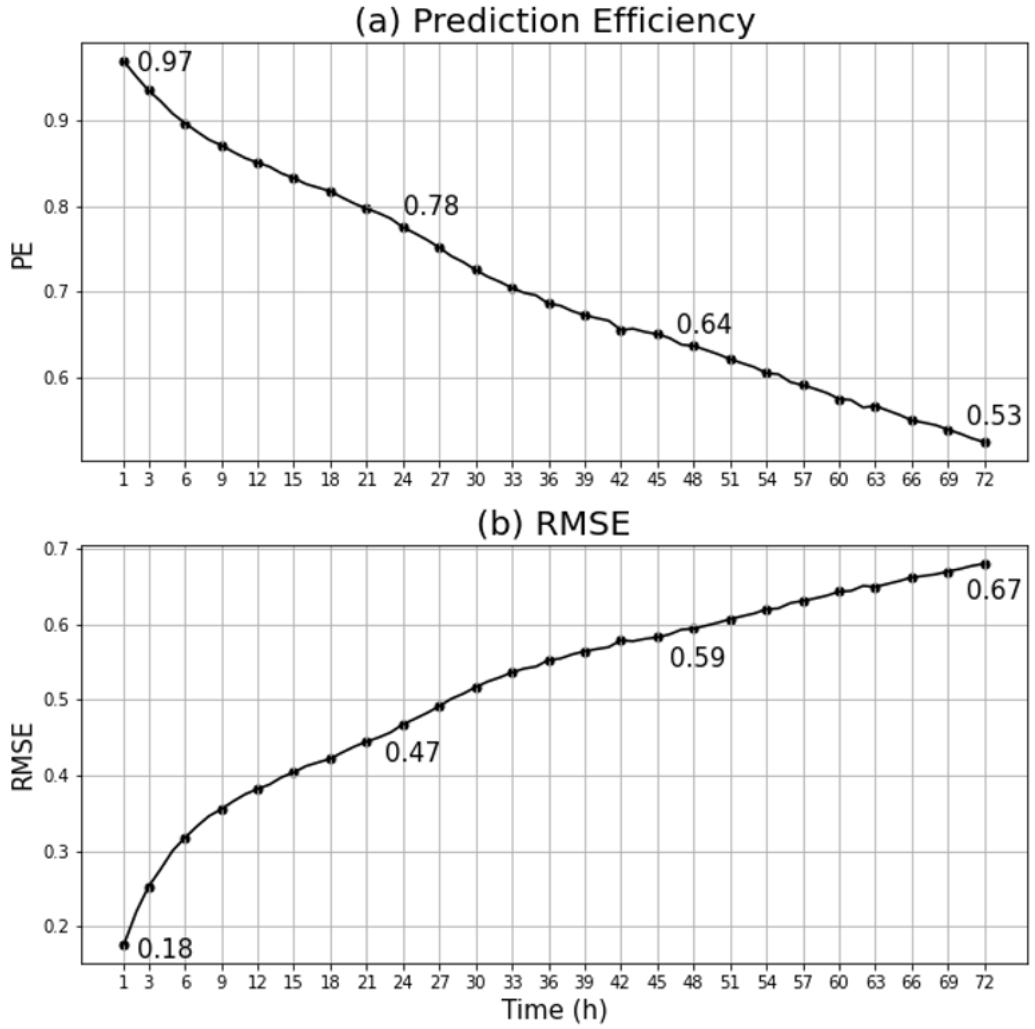

Figure 5. (a) shows prediction efficiency of our model for each time step, (b) shows RMSE. The values displayed in the graph are values for 1, 24, 48 and 72 hour prediction, respectively.

Figure 6 shows scatter plots of prediction values and real values of electron fluxes for 24 hours, 48 hours, and 72 hours ahead of prediction. The red line indicates a linear fitting line of the data, and the black dotted line is a one-to-one line. As the prediction date increases, the fitting line moves away from the one-to-one line, but it can be seen that all of them show a high correlation. As the electron fluxes increase, the model tends to underestimate, which appears to be due to the insufficient number of high-value data. In the upper left corner of each graph, we present the correlation coefficient (CC) between the observed values and the predicted values from the model, which is given by

$$CC = \frac{\sum(y_i - \bar{y})(f_i - \bar{f})}{\sqrt{\sum(y_i - \bar{y})^2(f_i - \bar{f})^2}}. \quad (5)$$

Table 1. Comparison of prediction efficiency with other hourly forecasting models

Model	Prediction time		Input data
	1 hour	24 hours	
Our model	0.97	0.78	GOES-15, 16
Persistence model	0.97	0.66	GOES-15, 16
Shin et al. (2016)	0.96	0.70	GOES-15
	0.93	0.68	GOES-13
Qian et al. (2020)	-	0.73	GOES-10

Our model has high CC values for all time forecasts, and in particular, the CC value of the 24 hours ahead prediction is quite high. In summary, in view of the metrics we obtained such as PE, RMSE, and CC, our model shows remarkable performance in predicting the relativistic electron fluxes.

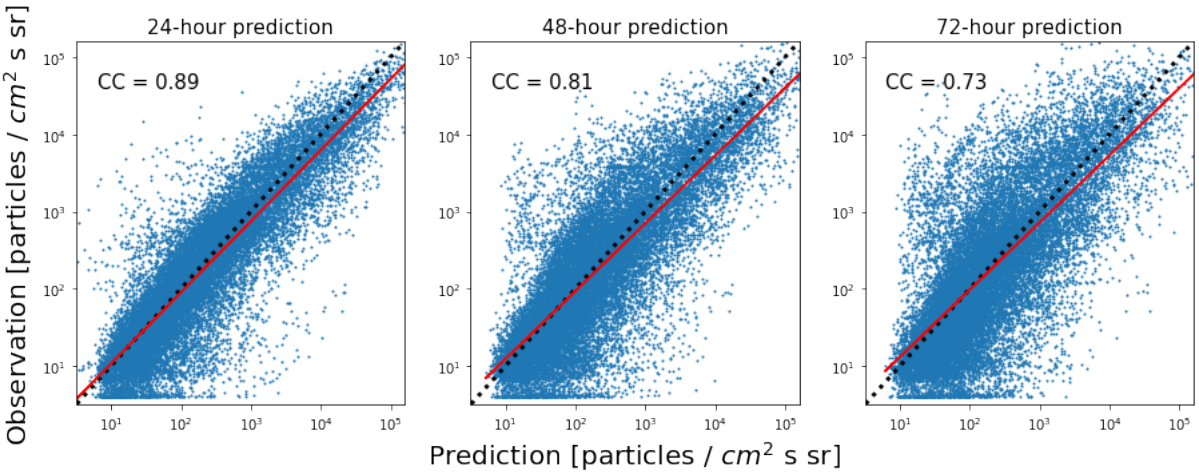

Figure 6. Scatter plots of prediction values (x-axis) and real values (y-axis) of electron fluxes for 24 hours, 48 hours, and 72 hours ahead prediction from left to right. The black dotted line is a one-to-one line, and the red line is a linear fitting line of the data. Correlation coefficient is 0.89, 0.81, and 0.73 for 24h, 48h, and 72h prediction, respectively.

5 Conclusion

In this study, we have developed a deep learning model for time series forecasting of electron fluxes at GEO. For this, we use solar wind data (speed, density, and temperature), IMF data ($|B|$ and B_z), geomagnetic indices (Kp and Dst), and electron flux data as input data. The electron fluxes are obtained from GOES-15 and GOES-16 satellites to consider the entire solar cycle period data, which cover from 2011 to 2021. We perform the cross-calibration of the two satellites' data. We have considered 3 deep learning methods, such as MLP, LSTM, and sequence-to-sequence. The best model is the MLP model, which has total 5 dense layers including output layer. The main results of the study are as follows. First, the model successfully predicts hourly electron fluxes over the next 72 hours, allowing us to see the changes in detail. Second, in view of the metrics such as PE, RMSE, and CC, the model shows better performance than the previous studies and the persistent model. Third, unlike a baseline model, which has only electron flux data as input, our model can predict sudden changes of electron fluxes associated with fast solar winds and interplanetary magnetic fields as well as their diurnal variations. It is noted that the model is able to predict a relatively long time (three day) with a high time resolution (one hour), which is contrasted with the conventional studies that predict the electron flux at a certain time and/or a short time period. The successful results of this study implies that the deep learning method can be applied to time series forecasting of various space weather events.

Acknowledgments

This work was supported by the Korea Astronomy and Space Science Institute (KASI) under the R&D program (project No. 2022-1-850-05) supervised by the Ministry of Science and ICT. We thank National Geophysical Data Center(NGDC; https://satdat.ngdc.noaa.gov/sem/goes/data/ for providing GOES electron flux data, and OMNIWeb service (https://omniweb.gsfc.nasa.gov/) for providing solar wind data and geomagnetic indices for this study. We acknowledge the community efforts devoted to developing the open-source packages that were used in this work.

References

Baker, D. (2000). The occurrence of operational anomalies in spacecraft and their relationship to space weather. *IEEE Transactions on Plasma Science*, *28*(6),

2007-2016. doi: 10.1109/27.902228

Baker, D., McPherron, R., Cayton, T., & Klebesadel, R. (1990). Linear prediction filter analysis of relativistic electron properties at 6.6 re. *Journal of Geophysical Research: Space Physics*, *95*(A9), 15133–15140.

Baker, D. N., Erickson, P. J., Fennell, J. F., Foster, J. C., Jaynes, A. N., & Verronen, P. T. (2018). Space Weather Effects in the Earth's Radiation Belts. , *214*(1), 17. doi: 10.1007/s11214-017-0452-7

Baker, D. N., Goldberg, R. A., Herrero, F. A., Blake, J. B., & Callis, L. B. (1993). Satellite and rocket studies of relativistic electrons and their influence on the middle atmosphere. *Journal of Atmospheric and Terrestrial Physics*, *55*(13), 1619-1628. doi: 10.1016/0021-9169(93)90167-W

Boynton, R. J., Balikhin, M. A., Sibeck, D. G., Walker, S. N., Billings, S. A., & Ganushkina, N. (2016, October). Electron flux models for different energies at geostationary orbit. *Space Weather*, *14*(10), 846-860. doi: 10.1002/2016SW001506

Denton, M. H., Thomsen, M. F., Jordanova, V. K., Henderson, M. G., Borovsky, J. E., Denton, J. S., ... Hartley, D. P. (2015, April). An empirical model of electron and ion fluxes derived from observations at geosynchronous orbit. *Space Weather*, *13*(4), 233-249. doi: 10.1002/2015SW001168

Fukata, M., Taguchi, S., Okuzawa, T., & Obara, T. (2002, July). Neural network prediction of relativistic electrons at geosynchronous orbit during the storm recovery phase: effects of recurring substorms. *Annales Geophysicae*, *20*(7), 947-951. doi: 10.5194/angeo-20-947-2002

Hartley, D. P., Denton, M. H., & Rodriguez, J. V. (2014, June). Electron number density, temperature, and energy density at GEO and links to the solar wind: A simple predictive capability. *Journal of Geophysical Research (Space Physics)*, *119*(6), 4556-4571. doi: 10.1002/2014JA019779

Hochreiter, S., & Schmidhuber, J. (1997). Long short-term memory. *Neural computation*, *9*(8), 1735–1780.

Horne, R. B., Glauert, S. A., Meredith, N. P., Boscher, D., Maget, V., Heynderickx, D., & Pitchford, D. (2013, April). Space weather impacts on satellites and forecasting the Earth's electron radiation belts with SPACECAST. *Space Weather*, *11*(4), 169-186. doi: 10.1002/swe.20023

Katsavrias, C., Aminalragia-Giamini, S., Papadimitriou, C., Sandberg, I., Jiggens, P., Daglis, I. A., & Evans, H. (2021, June). On the Interplanetary Parameter Schemes Which Drive the Variability of the Source/Seed Electron Population at GEO. *Journal of Geophysical Research (Space Physics)*, *126*(6), e28939. doi: 10.1029/2020JA028939

Kingma, D. P., & Ba, J. (2014). Adam: A Method for Stochastic Optimization. *arXiv e-prints*, arXiv:1412.6980.

Klambauer, G., Unterthiner, T., Mayr, A., & Hochreiter, S. (2017). Self-Normalizing Neural Networks. *arXiv e-prints*, arXiv:1706.02515.

Koons, H. C., & Gorney, D. J. (1991, April). A neural network model of the relativistic electron flux at geosynchronous orbit. , *96*(A4), 5549-5556. doi: 10.1029/90JA02380

Li, X. (2004, March). Variations of 0.7-6.0 MeV electrons at geosynchronous orbit as a function of solar wind. *Space Weather*, *2*(3), S03006. doi: 10.1029/2003SW000017

Li, X., Temerin, M., Baker, D. N., Reeves, G. D., & Larson, D. (2001). Quantitative prediction of radiation belt electrons at geostationary orbit based on solar wind measurements. , *28*(9), 1887-1890. doi: 10.1029/2000GL012681

Ling, A. G., Ginet, G. P., Hilmer, R. V., & Perry, K. L. (2010). A neural network-based geosynchronous relativistic electron flux forecasting model. *Space Weather*, *8*(9), S09003. doi: 10.1029/2010SW000576

Lyatsky, W., & Khazanov, G. V. (2008, August). A predictive model for relativistic electrons at geostationary orbit. , *35*(15), L15108. doi: 10.1029/2008GL034688

Miyoshi, Y., & Kataoka, R. (2008, February). Probabilistic space weather forecast of the relativistic electron flux enhancement at geosynchronous orbit. *Journal of Atmospheric and Solar-Terrestrial Physics*, *70*(2-4), 475-481. doi: 10.1016/j.jastp.2007.08.066

Onsager, T., Rostoker, G., Kim, H.-J., Reeves, G., Obara, T., Singer, H., & Smithtro, C. (2002). Radiation belt electron flux dropouts: Local time, radial, and particle-energy dependence. *Journal of Geophysical Research: Space Physics*, *107*(A11), SMP–21.

Qian, Y., Yang, J., Zhang, H., Shen, C., & Wu, Y. (2020, August). An Hourly

Prediction Model of Relativistic Electrons Based on Empirical Mode Decomposition. *Space Weather*, *18*(8), e02207. doi: 10.1029/2018SW002078

Reeves, G. D., Morley, S. K., Friedel, R. H. W., Henderson, M. G., Cayton, T. E., Cunningham, G., ... Thomsen, D. (2011, February). On the relationship between relativistic electron flux and solar wind velocity: Paulikas and Blake revisited. *Journal of Geophysical Research (Space Physics)*, *116*(A2), A02213. doi: 10.1029/2010JA015735

Rumelhart, D. E., Hinton, G. E., & Williams, R. J. (1986). Learning representations by back-propagating errors. *nature*, *323*(6088), 533–536.

Shin, D.-K., Lee, D.-Y., Kim, K.-C., Hwang, J., & Kim, J. (2016, April). Artificial neural network prediction model for geosynchronous electron fluxes: Dependence on satellite position and particle energy. *Space Weather*, *14*(4), 313-321. doi: 10.1002/2015SW001359

Sutskever, I., Vinyals, O., & Le, Q. V. (2014). *Sequence to sequence learning with neural networks.*

Turner, D. L., & Li, X. (2008). Quantitative forecast of relativistic electron flux at geosynchronous orbit based on low-energy electron flux. *Space Weather*, *6*(5), 05005. doi: 10.1029/2007SW000354

Ukhorskiy, A. Y., Sitnov, M. I., Sharma, A. S., Anderson, B. J., Ohtani, S., & Lui, A. T. Y. (2004, May). Data-derived forecasting model for relativistic electron intensity at geosynchronous orbit. , *31*(9), L09806. doi: 10.1029/2004GL019616

Vassiliadis, D., Klimas, A. J., Kanekal, S. G., Baker, D. N., & Weigel, R. S. (2002, November). Long-term-average, solar cycle, and seasonal response of magnetospheric energetic electrons to the solar wind speed. *Journal of Geophysical Research (Space Physics)*, *107*(A11), 1383. doi: 10.1029/2001JA000506

Wei, H. L., Billings, S. A., Surjalal Sharma, A., Wing, S., Boynton, R. J., & Walker, S. N. (2011, February). Forecasting relativistic electron flux using dynamic multiple regression models. *Annales Geophysicae*, *29*(2), 415-420. doi: 10.5194/angeo-29-415-2011

Wei, L., Zhong, Q., Lin, R., Wang, J., Liu, S., & Cao, Y. (2018). Quantitative Prediction of High-Energy Electron Integral Flux at Geostationary Orbit Based on Deep Learning. *Space Weather*, *16*(7), 903-916. doi: 10.1029/2018SW001829

Zhang, H., Fu, S., Xie, L., Zhao, D., Yue, C., Pu, Z., ... Luo, Z. (2020). Relativistic Electron Flux Prediction at Geosynchronous Orbit Based on the Neural Network and the Quantile Regression Method. *Space Weather*, *18*(9), e02445. doi: 10.1029/2020SW002445